Hybrid photonic crystal fiber for highly sensitive temperature measurement

Hybrid photonic crystal fiber for highly sensitive temperature measurement

Zhilin Xu[1, 2†], Baocheng Li[1†], Dora Juan Juan Hu[3*], Zhifang Wu[4], Slawomir Ertman[5], Tomasz Wolinski[5], Weijun Tong[6], and Perry Ping Shum[1, 2]

[1]School of Electrical and Electronic Engineering, Nanyang Technological University, 639798, Singapore

[2]CINTRA CNRS/NTU/THALES, UMI 3288, 639798, Singapore

[3]Institute for Infocomm Research, Agency for Science, Technology and Research (A*STAR), Singapore

[4]Fujian Key Laboratory of Light Propagation and Transformation, College of Information Science and Engineering, Huaqiao University, Xiamen 361021, China

[5]Faculty of Physics, Warsaw University of Technology, Warszawa, Poland

[6]Yangtze Optical Fibre and Cable Company Ltd (YOFC), Wuhan, 430074, China

†The authors contributed equally to this work

*Corresponding author: Dora Juan Juan Hu, jjhu@i2r.a-star.edu.sg

Abstract

A hybrid photonic crystal fiber (PCF) is proposed and demonstrated for highly sensitive temperature measurement. The hybrid PCF is formed by selectively infiltrating liquid crystal 5CB into the first ring of air holes around one silica core of a twin-core PCF (TCPCF). In the modified TCPCF, one silica core guides light with total internal reflection (TIR) mechanism, while the other silica core guides light through photonic bandgap (PBG) mechanism due to the infiltration of high refractive index 5CB. The co-existing of TIR and PBG waveguiding mechanisms in the TCPCF leads to a hybrid light guiding mechanism PCF, i.e. hybrid PCF. Theoretical analysis reveals that TIR-guided core mode, PBG-guided core modes and 5CB channel modes in the hybrid PCF can concurrently propagate and interfere with each other, which is further verified by experimental results. Besides, experimental investigation on temperature response of the hybrid PCF shows that the temperature sensitivities can be up to 4.91 nm/°C for nematic phase of 5CB, and -3.68 nm/°C for isotropic phase of 5CB, respectively. The proposed hybrid PCF is promising for applications of temperature-tunable optical filtering in optical fiber communication, sensing and laser systems.

Keywords: fiber optics sensors, liquid crystals, photonic crystal fibers

1. Introduction

Since it was firstly demonstrated in 1996 [1], photonic crystal fibers (PCFs) with air holes running along the length have been extensively explored for their broad potential applications [2-4]. In general, a PCF guides light either by modified total internal reflection (TIR) mechanism or photonic bandgap (PBG) mechanism, depending on the fiber structure [4, 5]. Hybrid PCFs with both TIR and PBG guiding mechanisms have also been reported using the germanium-doped silica rods around the silica core in holey structures [6]. After its first demonstration, hybrid PCFs based on different geometries have been proposed and analyzed. For example, L. Xiao et al presented a hybrid PCF with a hexagonal array of high-index rods and a line of air holes [7]. Ould-Agha et al proposed a structure of one ring of six high-index rods to extend the transmission band [8]. Andrea Cavanna et al designed a hybrid PCF consisting of an inner all-solid PBG structure and a conventional step-index solid-core PCF for phase matched third harmonic generation [9]. Because of the flexibility in controlling the mode properties and the phase matching conditions, these hybrid PCFs have been investigated for linear and nonlinear application such as broadband polarizers [10], optical amplifiers [11], optical sensors [12], supercontinuum generation [13,14] and third harmonic generation [9]. However, the hybrid PCFs mentioned above rely on special fiber designs, which is costly and requires sophisticated fabrication techniques.

The air holes running along the PCF allow researchers to flexibly tailor the mode properties of the fabricated PCF by selectively infiltrating liquid into air holes [15, 17]. Based on this idea, various optical fiber devices such as directional couplers [15, 16] and temperature sensors [17-21] have been demonstrated. Taking advantages of birefringence and

thermal tunable refractive indices (RIs) of liquid crystals (LCs), the PCFs with LCs inclusions open up a wide range of new possibilities for light propagation tuning properties in recent years [22, 23]. Particularly, the TIR-guided PCF can be converted into the PBG-guided PCF through filling air holes with high RI LCs [22-24]. For example, Alkeskjold et al demonstrated an all-optical modulation in a PCF filled with a dye-doped nematic LC [22]. Moreover, it is possible to achieve dynamic change of the guiding mechanism in PCF [23], or even obtain hybrid-mechanism guiding in which one polarization is TIR-guided whereas the orthogonal polarization is PBG-guided [24]. However, in this hybrid guiding PCF [24], the host material of PCF should be selected as a non-silica glass with RI between the extraordinary RI and ordinary RI of the LCs, which poses limitation to the practical applications.

In this paper, we propose a hybrid PCF formed by selectively infiltrating LC into a twin-core photonic crystal fiber (TCPCF). In the modified TCPCF, one silica core guides light with TIR mechanism, while the other silica core guides light through PBG mechanism due to the infiltration of LC with high RI. The co-existing of TIR and PBG waveguiding mechanisms thus leads to a hybrid PCF. Because of the thermal tunability of the LC, highly sensitive temperature measurement can be achieved by using the hybrid PCF. Mode dispersion curves of the TIR-guided core mode, PBG-guided core modes and the LC channel modes in the hybrid PCF will be thoroughly calculated and analyzed. Experimental investigation is also conducted to further explore the optical properties and temperature response of the hybrid PCF.

2. Working Principle

Schematic diagram of the designed hybrid PCF structure is presented in Fig. 1(a), where the first ring of air holes around the right silica core of a TCPCF is filled by high RI LC. In the modified TCPCF, the left silica core has a higher RI than the air holes cladding, so that light guiding is similar to classical propagation based on TIR guiding mechanism. In the right silica core, RI in the silica core is lower than RI in the LC cladding. Then, a PBG effect appears and only selected wavelengths can be propagated. Thereby, two different waveguiding mechanisms co-exist in the two silica cores of the modified TCPCF, forming a hybrid PCF structure. Because of the different light-guiding mechanisms, mode mismatching between the two cores is usually large, leaving light to propagate independently in each core, except at the phase matching wavelength λ_o, whereas coupling between the two cores occurs.

Besides, since the LC-filled voids can also be regarded as independent waveguides, the modes in the LC channels should also be considered. Due to the RIs of the LC channels are higher than RI of the silica background, the modes in the LC channels are guided by TIR mechanism. The coupling between the TIR-guided silica core mode and the 5CB channels modes will also take place in the hybrid PCF.

To have a deeper insight into the hybrid PCF, we use finite element method (FemSim, Rsoft) to analyze the modes properties. The TCPCF (YOFC Ltd.) used in this work has air holes diameters of 2.3 μm, pitches of 4 μm and outer diameter of 125 μm, as illustrate in Fig. 1(b). A type of nematic LC material, 4-pentyl-4'-cyanobiphenyl 5CB, with rod-like molecules, is employed because of its accessibility and high thermal tunability. For the nematic phase of 5CB at the temperature lower than the clearing temperature T_c, the temperature dependent anisotropic RIs of 5CB can be described by the four-parameters model [25]:

$$n_e(T) \approx A - BT + \frac{2(\Delta n)_o}{3}\left(1-\frac{T}{T_c}\right)^{\beta} \quad (1)$$

$$n_o(T) \approx A - BT - \frac{2(\Delta n)_o}{3}\left(1-\frac{T}{T_c}\right)^{\beta} \quad (2)$$

where n_e and n_o are the extraordinary RI and ordinary RI of 5CB respectively. T denotes temperature, and T_c is the clearing temperature of 5CB. $(\Delta n)_o$ is the birefringence of 5CB at $T = 0\,K$ and the exponent β is a material constant. For 5CB under investigation at wavelength of 589 nm, the parameters in the Eqs. (1) and (2) are $A = 1.7674$, $B = 5.79\times10^{-4}\,K^{-1}$, $(\Delta n)_o = 0.3505$, $T_c = 34.6\,°C$ and $\beta = 0.1889$, respectively [25]. By substituting the above parameters into Eqs. (1) and (2), RIs of 5CB under different temperature at the wavelength of 589 nm can be obtained, as plotted in Fig. 1(c). It should be noted that n_o takes dominating effect in modifying the wave-guiding properties of the PCF [24]. At first, n_o increases with the rise

of temperature. When the temperature is higher than the clearing temperature, n_e equals to n_o, the anisotropy vanishes, and 5CB turns into isotropic phase. The RI of 5CB in isotropic phase, n_{iso} decreases with the increasing temperature, as illustrated in Fig. 1(c).

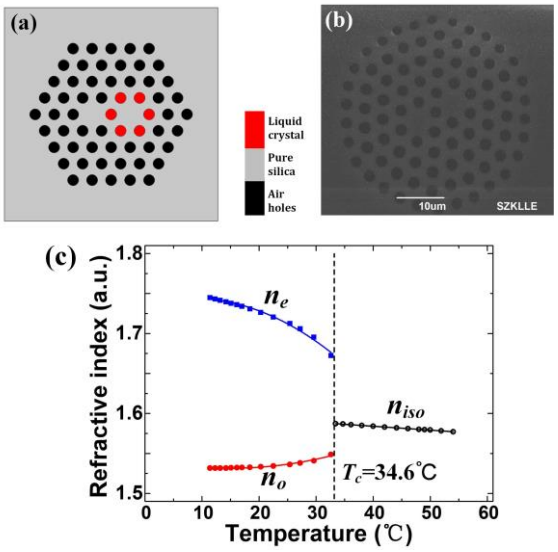

Fig. 1. (a) Schematic diagram of the designed hybrid PCF; (b) SEM picture of the TCPCF used in this work; (c) Temperature dependence of RI of 5CB at wavelength of 589 nm.

In the simulation, the RI of silica background in the TCPCF was determined by the Sellmeier's equation [26], while the RIs of 5CB were obtained by using the four-parameters model in Eqs. (1) and (2). At first, we calculate the dispersion curves of the TIR-guided core mode and PBG-guided core modes respectively, as presented in Fig. 2(a). It can be seen that for the TIR-guided core, RI of the fundamental mode linearly decreases with the increasing wavelength. For the PBG-guided core, the odd mode and the even mode have different dispersion performances due to the birefringence of 5CB. Dispersion curves of both the odd mode and the even mode have two crossing points with the dispersion curve of the TIR-guided core mode, at which the two cores attain phase matching. The crossing points are located at the wavelengths λ_0=1.00 μm (Point A) and λ_0=2.35 μm (Point D) for the odd mode, and at the wavelength of λ_0=1.19 μm (Point B) and λ_0=1.78 μm (Point C) for the even mode, respectively. The inset in Fig. 2(a) shows the *x*-polarization electric field distribution modes (E_x) at the crossing point C. At temperature of 39 °C, since the 5CB is in isotropic phase, the birefringence of 5CB disappears and the RI of 5CB steps to be around 1.5845, as indicated in Fig. 1(c). Then, the cross points between the dispersion curves of the PBG-guided core mode and that of the TIR-guided core mode are relocated to wavelengths of 0.939 μm and 1.498 μm, as marked as the points E and F in Fig. 2(a), respectively.

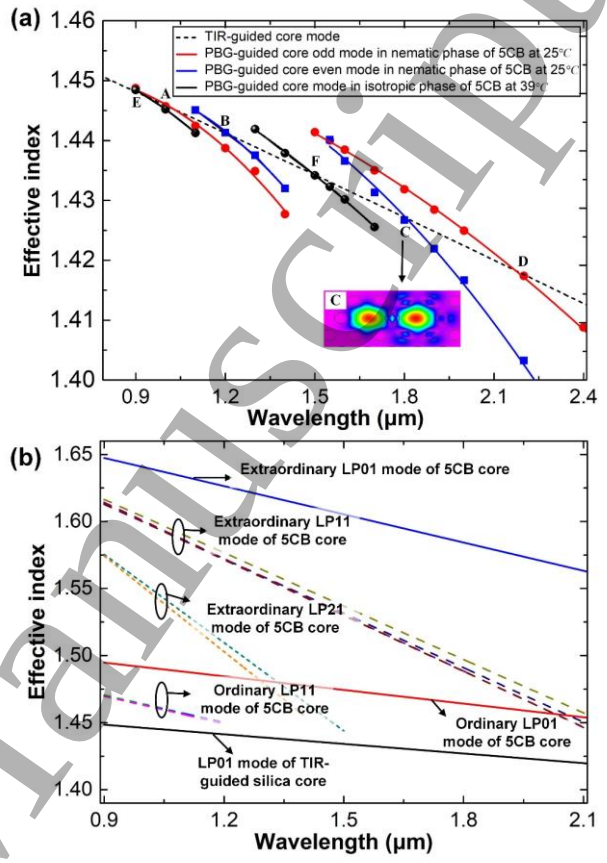

Fig. 2 (a) Dispersion curves of the TIR-guided core mode and the PBG-guided core modes in the hybrid PCF. Inset: *Ex* at the intersect point C (λ_0=1.78 μm). (b) The dispersion curves of the TIR-guided silica core mode and the 5CB channel modes.

The air holes filled with 5CB can naturally act as TIR-guided waveguides because the RIs of 5CB-filled-channels are higher than the RI of silica background. The dispersion curves of the modes in 5CB channels at temperature of 25 °C are calculated and shown in Fig. 2(b). The 5CB channels support 14 modes including 1 extraordinary LP_{01} mode, 4 degenerated extraordinary LP_{11} modes, 4 degenerated extraordinary LP_{21} modes, 1 ordinary LP_{01} mode and 4 degenerated ordinary LP_{11} modes. Therefore, in the hybrid PCF structure, the TIR-guided silica core mode, the PBG-guided silica core modes and the 14 modes in 5CB channels can concurrently propagate and interfere, inducing an interference spectrum. When the surrounding temperature of the hybrid PCF is changed, the RIs of the 5CB will be

changed due to the thermal optical effect. Then the effective RIs of modes in the PBG-guided core and the 5CB channels will be varied, causing the interference spectrum to shift, which is the basis of the temperature sensing in this study.

3. Experiment and results

For experimental demonstration, a 5CB-infiltrated hybrid PCF is prepared by using the method reported in our prior works [15-17]. Firstly, a clean TCPCF is cleaved and the flat end is focused under a microscope. Secondly, a tapered fiber dipping tiny droplets of UV glue (Thorlabs, NOA81) is placed under the microscope and moved to the top of the flat end of the TCPCF. Then, the slowly declined tapered fiber quickly transfers the UV glue onto the air holes to block them, but avoiding the selected air holes surrounding one of the two silica cores in TCPCF. After that, the blocked air holes are cured by exposing to UV light (Thorlabs, CS2010) for 90 seconds. Then, the blocking process of UV glue is completed. Subsequently, the blocked side of the TCPCF is placed into the 5CB solution, allowing 5CB to infiltrate the untouched air holes via capillary force. After cleaving the blocked side of the TCPCF, a hybrid PCF is then completed. The microscope image of the infiltration pattern is presented in Fig. 3(a), where the white spots show the air holes infiltrated with the 5CB and the black spots denote the un-infiltrated air holes. This indicates that the 5CB is fully filled into the PCF voids. It should be noted that although the fabricated sample is not exactly the same with the theoretically proposed one, the operating principle of the hybrid PCF will not be affected because the optical properties of the hybrid PCF is mainly affected by the holes of the first layer [27].

After fabrication, both sides of the hybrid PCF are spliced to a section of single mode fiber (SMF) by using a fusion arc splicer (Fujikura, FSM-100P+) with customer settings. The fusion splicing between the hybrid PCF and the SMF is center alignment. An 80μm offset between the hybrid PCF-SMF joint and the splicer electrodes is introduced to reduce the heat received at the hybrid PCF side, which avoids collapse of holes in the hybrid PCF. A pre-fusion and two arcs with parameters shown in Table 1 are applied in the experiment to form a neat and a mechanically strong splicing point without bubble and collapsing, as illustrated in Fig. 3 (b). In the fabricated SMF-hybrid PCF-SMF sample, the length of the hybrid PCF is about 5 cm. Then, the sample is placed in a temperature controller (HC Photonics Corp., TC038-PC) with temperature control accuracy of 0.1 °C to investigate its transmission spectra at different temperature, as displayed in Fig. 3(c). In the experiment, the temperature is controlled from 27 °C to 46 °C in step of 0.2 °C. The broadband light source (Infinon Research, IRBL-11111-F,) is with wavelength range from 1300 nm to 1620 nm and the optical spectrum analyzer (Yokogawa, AQ6370C) is with resolution of 0.1nm.

Table 1 The arc parameters in the splicing process

	Arc power (bit)	Arc time (ms)
Prefusion	256	20
1st arc	196	500
2nd arc	206	600

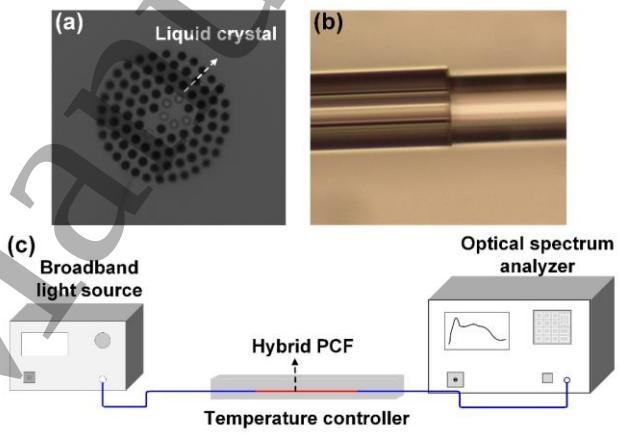

Fig. 3. (a) Microscope picture of the fabricated hybrid PCF; (b) Detailed view of the splicing point between the hybrid PCF and SMF; (c) Experimental setup for temperature sensing.

Transmission spectra of the hybrid PCF at 30.2 °C in nematic phase of 5CB and at 39.2 °C in isotropic phase of 5CB are given in Fig. 4. At the temperature of 30.2 °C, broadband interference fringes within wavelength range from 1400 nm to 1600 nm can be observed, which results from the interferences among the TIR-guided core mode, the PBG-guided core mode and the multiple modes in the 5CB channels. The extinction ratios of the fringes are mostly around 10 dB. The absence of obvious notch in Fig. 4 is because the TIR-guided core mode and the PBG-guided core modes do not attain phase matching within the available light source wavelength range.

At the temperature of 39.2 °C, intensity of the transmission spectrum increases by almost 10dB compared

with that of 30.2 °C. The interference fringes at wavelength below 1500 nm almost disappear, while the fringes from 1500 nm to 1600 nm become more sparse and clear. The above observations can be attributed to the better uniform alignment of 5CB in isotropic phase [28]. According to the analysis in Fig. 2 (a), the TIR-guided core mode and the PBG-guided core mode can attain phase matching at wavelength of 1498 nm. Indeed, we can observe a small notch around 1504.5 nm. The slight difference of the phase matching wavelength can be explained by the difference between the simulation assumption and the experiment conditions. The small extinction ratio of the notch is due to the unbalanced optical intensities of the TIR-guided core mode and the PBG-guided core mode which results from the existence of other 5CB channel modes.

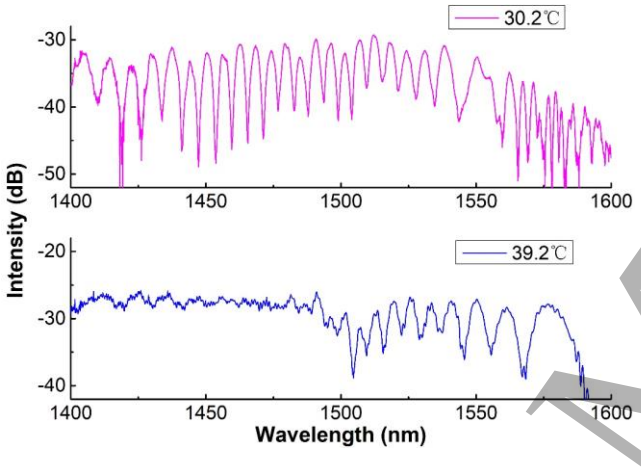

Fig. 4. Transmission spectra of the hybrid PCF at (a) 30.2 °C in nematic phase of 5CB and (b) 39.2 °C in isotropic phase of 5CB.

Furthermore, temperature response of the hybrid PCF is investigated. Figures 5(a) and 5(b) present the experimental results for the nematic phase of 5CB, i.e. temperature lower than the clearing temperature of 34.6 °C. We can be see from Fig. 5(a) that the transmission spectrum shifts to longer wavelength with the rising temperature. As mentioned above, n_o takes dominating effect in modifying the wave-guiding properties of the PCF. When the temperature is below the clearing temperature, n_o increases as the temperature rises. This will increase the difference of effective index between the TIR-guided core mode and PBG-guided core modes, as well as between the TIR-guided core mode and the 5CB channel modes, causing the transmission spectrum to be red shifted [17]. We choose 2 dips labelled in Fig. 5(a) as indicators to discuss the temperature responses of different dips in the transmission spectrum. The dependences of the wavelengths on the temperature in both heating and cooling processes are presented in Fig. 5(b). For Dip 1, the temperature sensitivities are 4.58 nm/°C for the heating process and 4.91 nm/°C for the cooling process. For Dip 2, the temperature sensitivities are 4.45 nm/°C for the heating process and 4.54 nm/°C for the cooling process.

Figures 5(c) and 5(d) present the experimental results for the condition of isotropic phase of 5CB, i.e. temperature higher than the clearing temperature of 34.6 °C. It can be seen that the transmission spectrum shifts to shorter wavelength with the rise of temperature, which can be attributed that n_{iso} decreases with the rise of temperature. Similarly, we choose 2 dips as indicators to characterize the temperature response. For Dip 3, the temperature sensitivities are -3.37 nm/°C for the heating process and -3.315 nm/°C for the cooling process. For Dip 4, the temperature sensitivities are -3.68 nm/°C for the heating process and -3.35 nm/°C for the cooling process. The existence of hysteresis between the temperature rising and declining processes mainly results from the thermal expansion of the 5CB, which causes 5CB not to return to the original state after cooling [25].

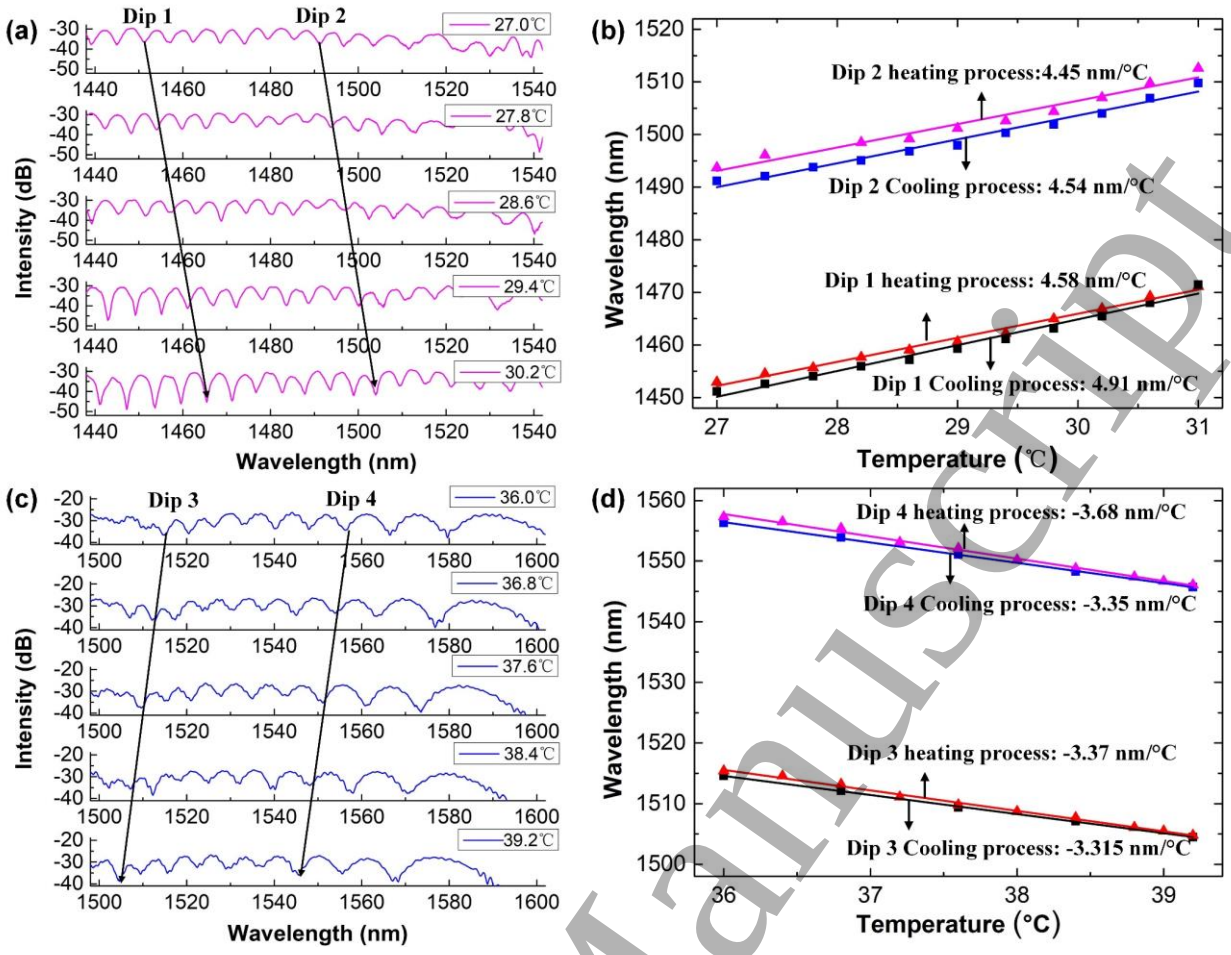

Fig. 5. Experimental results for temperature response of the hybrid PCF. (a) and (b) are results for temperature below the clearing temperature: (a) Transmission spectra of the hybrid PCF under different temperature; (b) dependence of resonant wavelengths of Dip 1 and Dip 2 on the temperature. (c) and (d) are results for temperature higher than the clearing temperature: (c) Transmission spectra of the hybrid PCF under different temperature; (d) dependence of resonant wavelengths of Dip 3 and Dip 4 on the temperature.

4. Conclusion

In conclusion, we have proposed and demonstrated a hybrid PCF by selectively infiltrating the liquid crystalline material 5CB into the first ring of air hole around one silica core of a TCPCF. Theoretical analysis reveals that the TIR-guided core mode, PBG-guided core modes and 5CB channel modes in the hybrid PCF can concurrently propagate and interfere with each other. The strong thermal dependence of the 5CB causes the temperature dependent interference spectrum, endowing the hybrid PCF with high temperature sensitivity. Experimental results show that the temperature sensitivities can be up to 4.91 nm/°C for nematic phase of 5CB and -3.68 nm/°C and isotropic phase of 5CB, respectively. The proposed hybrid PCF has good potential for temperature-tunable optical filtering in optical fiber communication, sensing and laser systems.

Acknowledgments

This work is partially supported by National Research Foundation Singapore (NRF) (NRF-CRP13-2014-05), National Natural Science Foundation of China (11774102), the Scientific Research Funds and Promotion Program for Young and Middle-aged Teacher in Science & Technology Research of Huaqiao University (ZQN-YX504, 17BS412), Open Fund of IPOC (BUPT) and Singapore Ministry of Education Academic Research Fund Tier 1 (RG89/16).

References

[1] J. C. Knight, T. A. Birks, P. St. J. Russell, and D. M. Atkin, "All-silica single-mode optical fiber with photonic crystal cladding," *Opt. Lett.*, vol. 21, no. 19, pp.1547-1549, Oct. 1996.

[2] P. Russell, "Photonic crystal fibers," *Science*, vol. 299, no. 5605, pp. 358-362, Jan. 2003.

[3] J. C. Knight, "Photonic crystal fibres," *Nature*, vol. 424, pp. 848-851, Aug. 2003.

[4] J. Villatoro, J. Zubia, "New perspectives in photonic crystal fibre sensors," *Opt. Laser Technol.*, vol. 78, pp. 67–75, Apr. 2016.

[5] S. Ertman, P. Lesiak, T. R. Woli´nski, "Optofluidic photonic crystal fiber-based sensors," *J. Lightwave Technol.*, vol. 35, no. 16, pp. 3399-3405, Aug. 2017.

[6] A. Cerqueira S. Jr., F. Luan, C. M. B. Cordeiro, A. K. George, and J. C. Knight, "Hybrid photonic crystal fiber," *Opt. Express,* vol. 14, no. 2, pp. 926-931, Jan. 2006.

[7] L. Xiao, W. Jin, M.S. Demokan, "Photonic crystal fibers confining light by both index-guiding and bandgap-guiding: hybrid PCFs," *Opt. Express*, vol. 15, no. 24, pp. 15637-15647 (2007)

[8] Y. Ould-Agha, A. Bétourné, O. Vanvincq, G. Bouwmans, and Y. Quiquempois, "Broadband bandgap guidance and mode filtering in radially hybrid photonic crystal fiber," *Opt. Express,* vol. 20, no. 6, pp. 6746-6760, Mar. 2012.

[9] A. Cavanna, F. Just, X. Jiang, G. Leuchs, M. V. Chekhova, P. St.J. Russell, and N. Y. Joly, "Hybrid photonic-crystal fiber for single-mode phase matched generation of third harmonic and photon triplets," *Optica,* vol. 3, no. 9, pp. 952-955, Sep. 2016.

[10] S. Arismar Cerqueira Jr., D. G. Lona, I. de Oliveira, H. E. Hernandez-Figueroa, H. L. Fragnito, "Broadband single-polarization guidance in hybrid photonic crystal fibers," *Opt. Lett.* vol. 36, no. 2, pp. 133 – 135, Jan. 2011.

[11] T. T. Alkeskjold, "Large-mode-area ytterbium-doped fiber amplifier with distributed narrow spectral filtering and reduced bend sensitivity," *Opt. Express,* vol. 17, no. 19, pp. 16394 – 16405, Aug. 2009.

[12] M. Pang, L.M. Xiao, W. Jin, S. Arismar Cerqueira Jr., "Birefringence of hybrid PCF and its sensitivity to strain and temperature," *J. Lightwave Technol.*, vol. 30, no. 10, pp. 1422 – 1432, May 2012.

[13] V. Pureur, J. M. Dudley, "Nonlinear spectral broadening of femtosecond pulses in solid-core photonic bandgap fibers," *Opt. Lett.* vol. 35, no. 16, pp. 2813 – 2815, Aug. 2010.

[14] D. R. Austin, C. M. de Sterke, B. J. Eggleton, T. G. Brown, "Dispersive wave blue-shift in supercontinuum generation," *Opt. Express,* vol. 14, no. 25, pp. 11997–12007, Dec. 2006.

[15] D. J. J. Hu, P. P. Shum, J. L. Lim, Y. Cui, K.a Milenko, Y. Wang, and T. Wolinski, "A compact and temperature-sensitive directional coupler based on photonic crystal fiber filled with liquid crystal 6CHBT," *IEEE Photon. J.*, vol. 4, no. 5, pp. 2010-2016, Oct. 2012.

[16] D. J. J. Hu, J. L. Lim, Y. Cui, K. Milenko, Y. Wang, P. Shum, and T. Wolinski, "Fabrication and characterization of a highly temperature sensitive device based on nematic liquid crystal-filled photonic crystal fiber," *IEEE Photon. J.,* vol. 4, no. 5, pp. 1248–1255, Oct. 2012.

[17] Z. Xu, J. Lim, D. J. J. Hu, Q. Sun, R. Y. N. Wong, K. Li, M. Jiang, and P. P. Shum, "Investigation of temperature sensing characteristics in selectively infiltrated photonic crystal fiber," *Opt. Express,* vol. 24, no. 2, pp. 1699-1707, Jan. 2016.

[18] J. Ma, H. H. Yu, X. Jiang, and D. S. Jiang, "High-performance temperature sensing using a selectively filled solid-core photonic crystal fiber with a central air-bore," *Opt. Express,* vol. 25, no. 8, pp. 9406-9415, Apr. 2017.

[19] X. G. Li, X. Zhou, Y. Zhao, R. Q. Lv, "Multi-modes interferometer for magnetic field and temperature measurement using Photonic crystal fiber filled with magnetic fluid," *Opt. Fiber Technol.*, vol. 41, pp. 1-6, Mar. 2018.

[20] Y. Zhao, Q. L. Wu, and Y. N. Zhang, "Theoretical analysis of high-sensitive seawater temperature and salinity measurement based on C-type micro-structured fiber," *Sensor Actuat. B-Chem.*, vol. 258, pp. 822-828, Apr. 2018.

[21] P. Yang, J. Hou, Y. Zhang, Z. Huang, R. Xiao, and Q. Lu, "Temperature sensing using the bandgap-like effect in a selectively liquid-filled photonic crystal fiber," *Opt. Lett.*, vol. 38, no. 3, pp. 263-265, Feb. 2013.

[22] T. T. Alkeskjold, J. Lægsgaard, A. Bjarklev, D. S. Hermann, Anawati, J. Broeng, J.Li, and S. T. Wu, "All-optical modulation in dye-doped nematic liquid crystal photonic bandgap fibers," *Opt. Express,* vol. 12, no. 24, pp. 5857-5871, Nov. 2004.

[23] T. R.Wolinski, K, Szaniawska, S. Ertman, P. Lesiak, A. WDomanski, R. Dabrowski, E. Nowinowski-Kruszelnicki, and J. Wojcik, "Influence of temperature and electrical fields on propagation properties of photonic liquid-crystal fibres," *Meas. Sci. Technol.*, vol. 17, no. 5, pp. 985–991, Apr. 2006.

[24] J. Sun and C. C. Chan, "Hybrid guiding in liquid-crystal photonic crystal fibers," *J. Opt. Soc. Am. B,* vol. 24, no. 10, pp. 2640-2646, Oct. 2007.

[25] J. Li, S. Gauza, and S. T. Wu, "Temperature effect on liquid crystal refractive indice," *J. Apl. Phys.*, vol. 96, no. 1, pp. 19-24, Jul. 2004.

[26] P. Klocek, Handbook of Infrared Optical Materials, Marcel Dekker, New York,1991.

[27] A. Bétourné, V. Pureur, G. Bouwmans, Y. Quiquempois, L. Bigot, M. Perrin, M. Douay, "Solid photonic bandgap fiber assisted by an extra air-clad structure for low-loss operation around 1.5 μm," *Opt. Express*, vol. 15, no. 2, pp. 316-324, Oct. 2006.

[28] K. A. Rutkowska, A. Kozak, and K. Orzechowski, "Chromatic dispersion measurements of selected liquid crystalline materials for integrated optics applications," in *IOS*, Szczyrk, 2016, pp. 100340J.